

The Development of a High-Power, Low-Frequency Underwater Acoustic Source for Use in a Deep-Towed Geophysical Array System

A. M. YOUNG, A. C. TIMS, AND T. A. HENRIQUEZ

*Underwater Sound Reference Detachment
P.O. Box 8337
Orlando, FL 32856*

November 15, 1982



NAVAL RESEARCH LABORATORY
Washington, D.C.

Approved for public release; distribution unlimited.

SECURITY CLASSIFICATION OF THIS PAGE (When Data Entered)

REPORT DOCUMENTATION PAGE		READ INSTRUCTIONS BEFORE COMPLETING FORM
1. REPORT NUMBER NRL Report 8633	2. GOVT ACCESSION NO.	3. RECIPIENT'S CATALOG NUMBER
4. TITLE (and Subtitle) THE DEVELOPMENT OF A HIGH-POWER, LOW-FREQUENCY UNDERWATER ACOUSTIC SOURCE FOR USE IN A DEEP-TOWED GEOPHYSICAL ARRAY SYSTEM	5. TYPE OF REPORT & PERIOD COVERED Final report	
	6. PERFORMING ORG. REPORT NUMBER	
7. AUTHOR(s) A. M. Young, A. C. Tims, and T. A. Henriquez	8. CONTRACT OR GRANT NUMBER(s)	
9. PERFORMING ORGANIZATION NAME AND ADDRESS Naval Research Laboratory Underwater Sound Reference Detachment P.O. Box 8337, Orlando, FL 32856	10. PROGRAM ELEMENT, PROJECT, TASK AREA & WORK UNIT NUMBERS 61153N 59-0597-02	
11. CONTROLLING OFFICE NAME AND ADDRESS Office of Naval Research Naval Ocean Research and Development Activity	12. REPORT DATE November 15, 1982	
	13. NUMBER OF PAGES 22	
14. MONITORING AGENCY NAME & ADDRESS (if different from Controlling Office)	15. SECURITY CLASS. (of this report) UNCLASSIFIED	
	15a. DECLASSIFICATION/DOWNGRADING SCHEDULE	
16. DISTRIBUTION STATEMENT (of this Report) Approved for public release; distribution unlimited.		
17. DISTRIBUTION STATEMENT (of the abstract entered in Block 20, if different from Report)		
18. SUPPLEMENTARY NOTES This transducer was developed for use in the Naval Oceanographic Research and Development Activity's deep-towed geophysical array system.		
19. KEY WORDS (Continue on reverse side if necessary and identify by block number) High-power Low-frequency Helmholtz resonator Equivalent circuit analysis		
20. ABSTRACT (Continue on reverse side if necessary and identify by block number) A high-power, low-frequency acoustic source in the form of a Helmholtz resonator, has been developed for use in the deep ocean in a geophysical application. The successful development of the transducer was accomplished through the use of equivalent circuit analysis and the construction/evaluation of a scale model. The transducer has been evaluated and performed well in the 250 to 500-Hz frequency range in both a shallow-water acoustic measurements facility and in the ocean to depths of over 2000 m.		

DD FORM 1473
1 JAN 73EDITION OF 1 NOV 65 IS OBSOLETE
S/N 0102-014-6601

SECURITY CLASSIFICATION OF THIS PAGE (When Data Entered)

CONTENTS

INTRODUCTION	1
DESIGN CONSIDERATIONS	2
ANALYSIS OF THE SUBJECT TRANSDUCER	5
ELECTROMECHANICAL DESIGN	9
ACOUSTIC EVALUATION OF THE G62 TRANSDUCER	14
CONCLUSIONS	17
ACKNOWLEDGMENTS	17
REFERENCES	17
APPENDIX A – Determination of Values for the Elements of the Equivalent Circuit	18

THE DEVELOPMENT OF A HIGH-POWER, LOW-FREQUENCY UNDERWATER ACOUSTIC SOURCE FOR USE IN A DEEP-TOWED GEOPHYSICAL ARRAY SYSTEM

INTRODUCTION

"The Navy's interest in the lower region of the acoustic frequency domain has increased the need for more definitive models of the ocean's subbottom as a transmission media that refracts, diffracts, diffuses and dissipates, as well as reflects, acoustic energy. A multichannel array system towed near the bottom in the deep ocean provides the capability to determine the detailed geophysical character of the subbottom structure and thus provides the high-resolution geoacoustic input parameters required for modeling." That conclusion, by the Naval Ocean Research and Development Activity (NORDA), was the impetus for a program, initiated in 1978, to develop a deep-towed geophysical array system (DTAGS). As part of this program, the Underwater Sound Reference Detachment (USRD) of the Naval Research Laboratory assessed the state of the art in high-power, low-frequency acoustic sources for the deep-towed application with the objective to recommend the most technically feasible approach to satisfy the requirements summarized in Table 1. The conclusion of that work was that a large Helmholtz resonator, using piezoelectric ceramic as the transduction mechanism, was the recommended approach [1]. Further engineering studies and analyses were conducted during 1980, and the detailed design and fabrication of the transducer were completed during 1981. The transducer was installed in an experimental DTAGS system and performed extremely well during evaluation measurements conducted at sea in December 1981. This report documents the development of the transducer.

Table 1 — Deep-Towed Sound Source Requirements.

Sound Pressure Level	204 dB re $a \mu\text{Pa}$ at 1 m
Frequency	< 500 Hz
Bandwidth	> 200 Hz
Maximum Dimensions	0.6-m dia; 1.8-m long
Desired Weight	460 kg
Maximum Operating Depth	6000 m
Signal Characteristics	
Maximum Pulse Length	5 m sec (pulsed cw) 500 m sec (pulsed fm)
Maximum Repetition Rate	1 pulse per 15 sec

DESIGN CONSIDERATIONS

Virtually all high-power, low-frequency acoustic sources designed to operate over an appreciable bandwidth will be large, heavy, and relatively expensive. The undesirable characteristics inherent in these transducers, however, are not the products of poor design, but instead may be shown to be direct results of the physics of the radiation problem itself. Several transduction mechanisms, in different design configurations, are capable of producing the required sound pressure level over the frequency range specified for the deep-towed application. Most of these designs, however, require some form of depth compensation and/or pressure release for the interior of the radiator which either limits the operational depth capability of the device or greatly increases its complexity. Aside from the obvious constraints of output power and bandwidth, the design of the required transducer will be determined by the trade-off between achieving the operational depth capability and the restraints on size and weight. The ideal device would be one which would meet all of the electroacoustic requirements while operating independently of water depth.

The search for the ideal solution naturally leads to the consideration of design configurations which can be *free-flooded* (i.e., configurations where no pressure differential exists across any portion of the transducer due to the surrounding hydrostatic pressure). The Helmholtz resonator basically consists of a closed rigid cavity coupled to the external medium through an opening or orifice, and as such is a "free-flooded" device. Helmholtz resonators have been used as filter elements in air acoustics and as narrow bandwidth sources in underwater acoustics. The application under consideration here, however, is the use of a Helmholtz resonator to increase the low-frequency output of a piezoelectric ceramic radiator as shown in Fig. 1. As shown in the figure, well below the frequency of its first resonance, a piezoelectric radiator normally has a positive 12-dB-per-octave slope in the output sound pressure level per volt as a function of increasing frequency. If, however, the ceramic element is used in a configuration where one of its surfaces radiates directly into the unbounded medium and the other surface radiates into the fluid-filled cavity of a Helmholtz resonator, there will be a resultant increase in the output sound pressure level at the Helmholtz resonance frequency.

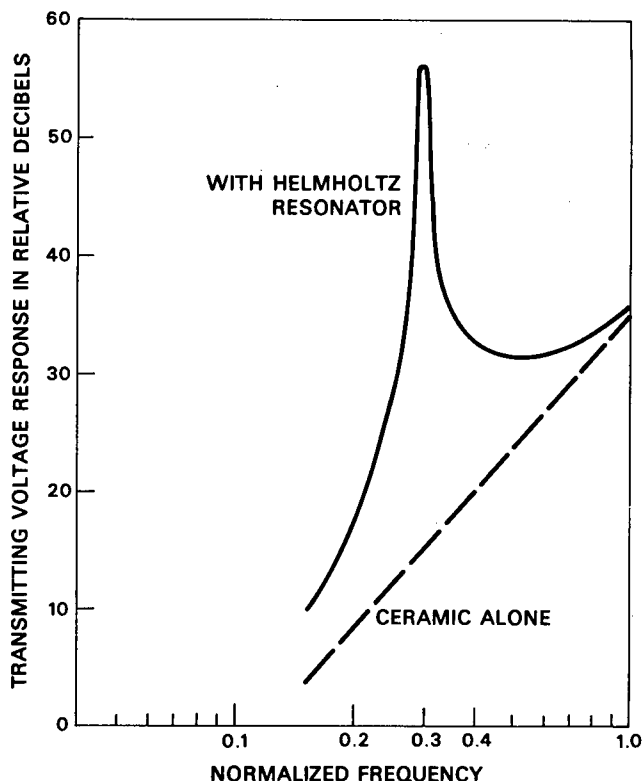
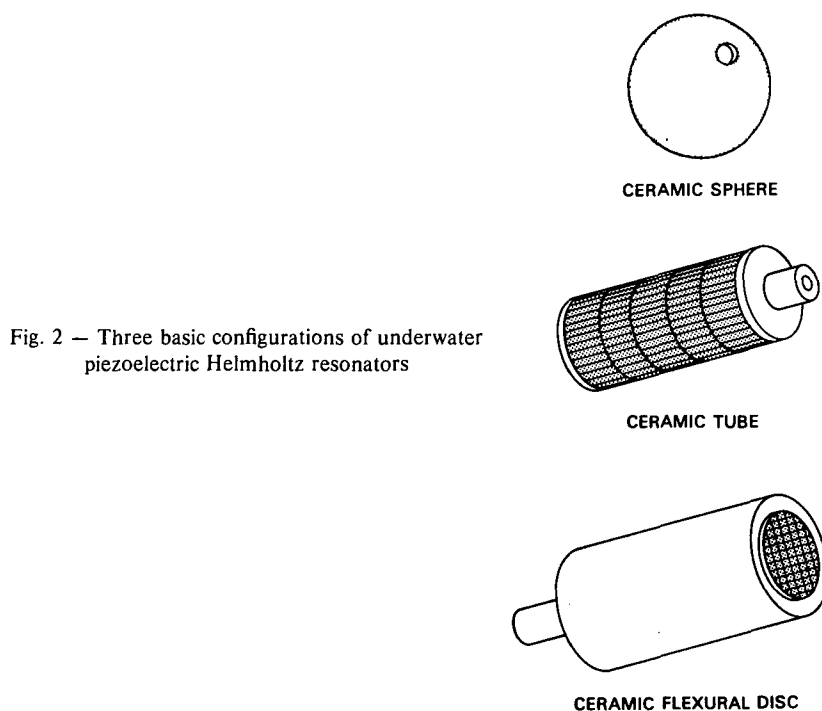


Fig. 1 — Transmitting voltage response of a fluid-filled piezoelectric ceramic tube with and without a Helmholtz resonator (orifice in one end)

In this type of transducer, the ceramic radiator could generally be in the form of one of three basic configurations in which all or part of the Helmholtz cavity is formed by the ceramic. These three configurations are shown in Fig. 2. The most simple configuration is that of a piezoelectric ceramic sphere where the interior volume of the sphere forms the Helmholtz cavity. This design, however, would not generally be considered feasible for the frequencies desired because the mosaic construction required for large sizes makes the sphere relatively fragile and expensive. In the second configuration, a piezoelectric ceramic tube forms all but the ends of a cylindrical cavity. The large sizes required by low-frequency applications dictate that the ceramic tube be fabricated from a stack of segmented ceramic rings as shown in the figure. In this configuration, to assure that the ceramic remains in compression, the rings must be radially prestressed by wrapping them with a glass-fiber/epoxy composite. The ring segments may be either radially or circumferentially poled although poling thickness limitations generally make circumferential poling preferable. The third configuration consists of a cylindrical metal housing with a ceramic flexural disc at one end. The flexural disc may be either bilaminar or trilaminar in construction; that is, with a mosaic of piezoelectric ceramic laminated to either one or both sides of a metal disc. Of the two configurations considered feasible for low-frequency applications, each has advantages over the other dependent primarily upon geometry constraints. When the requirements do not constrain the diameter, the flexural disc would be the most efficient radiator; if the diameter is constrained, however, the segmented ceramic rings would become the preferred radiator. In the case of NORDA's requirements, the maximum allowable diameter is more constrained than is the length, making the segmented ceramic rings the better choice.



The principle of the Helmholtz resonator appears to have been first applied to increase the low-frequency acoustic output of piezoelectric ceramic transducers approximately 8 to 12 years ago [2,3]. Neither of these previous applications, however, were for transducers with the requirements of output sound pressure level, depth, and frequency range demanded by the NORDA system. The application of the Helmholtz resonator to lower frequency, higher power requirements has been addressed in some detail and at least one experimental model evaluated [4,5]. Although operable over nearly the same frequency range as required by the NORDA application, this experimental model was designed for use at a much shallower depth and some 30 to 40 dB less acoustic output.

From the simple equation for the resonance frequency of a Helmholtz resonator

$$f_r = \frac{1}{2\pi} \sqrt{\frac{1}{C_c M_A}}, \quad (1)$$

where C_c is the compliance of the cavity and M_A is the inertance of the orifice; it would appear to be possible to design a device for operation at low frequencies with a small orifice radius and small cavity volume. However, internal losses increase with decreasing orifice size and cavity volume. Decreasing the cavity volume also decreases the volume of ceramic in the transducer and, therefore, the maximum available volume velocity. In other words, the orifice size and cavity volume may be decreased only at the expense of a lower acoustic output power capability. Obviously then, for the high-power application being considered, it is desirable to maximize the orifice size and cavity volume within the size and weight restraints of the specifications. Since the most severely restrained dimension is the diameter of the transducer, this may be accomplished by setting the orifice diameter equal to the maximum inside diameter of the cavity and varying the cavity length to achieve the desired resonance frequency. This approach will also have the advantage of minimizing the viscous losses in the orifice since its diameter will be at the maximum allowable dimension.

In reality, the Helmholtz resonance frequency for a given orifice inertance is determined not only by the compliance of the cavity, but by the compliance of the total system. That is, the resonance frequency is influenced by other mechanical compliances in the system such as the compliance of the piezoelectric ceramic driver, C_d . Woollett [4] identified the relationship between the cavity compliance, C_c , and the driver compliance, C_d , as an important design parameter and defined it as

$$\alpha = \frac{C_d}{C_d + C_c}. \quad (2)$$

It can be shown that for a given design, the output power is proportional to the factor $(1 - \alpha)^2$ while the viscous loss in the cavity is inversely proportional to $(1 - \alpha)$. Therefore, if the compliance of the driver becomes large in relation to the compliance of the cavity, the output power will decrease and the viscous loss in the cavity will increase. Since in the conceptual design being developed for NORDA's specifications, both the compliances of the driver and the cavity are directly proportional to the cavity length, the length of the cavity has no effect on α . The value of α is, however, dependent upon the mean diameter of the ceramic rings and their wall thicknesses. The value of α for this application will be determined by the compromise between the acoustic requirements and the limitations of geometry and weight.

The radiated power at the Helmholtz resonance frequency is, of course, determined in large part by the Q of the device. There is maximum, or lossless, Q associated with any Helmholtz resonator and it is primarily dependent upon the size of the transducer. That is, in general, for a given frequency, the larger the transducer becomes, the higher will be its Q , or sharpness of resonance. The Q actually obtained in practice, however, is strongly dependent upon internal losses in the system, primarily viscous losses in the cavity and orifice. In this case, since the orifice diameter and the cavity diameter are equal, the orifice length is zero and the only viscous losses are those associated with fluid flow in the cavity.

A second parameter which affects the maximum radiated power at the Helmholtz resonance frequency is the fracture stress of the ceramic rings. If the Q of the system is high, the pressure inside the cavity can cause the fracture stress of the ceramic to be exceeded at high drive levels. The result would be a catastrophic failure of the rings. The maximum allowable sound pressure level that can be obtained near the resonance frequency may be determined from the geometry of, and the material used to construct, the ceramic driver.

A review of the design considerations discussed, with respect to the requirements listed in Table 1, leads to a conceptual design for a transducer like that shown in Fig. 3. To afford mechanical protection for the ceramic rings, and at the same time keep the interior of the cavity free from obstructions, an exterior support framework is envisioned. This *exoskeleton* would consist of a rigid backplate to close one end of the cavity, metal spacer rings to support the ceramic, a metal end ring for the orifice end of the transducer, and the hardware necessary to fasten the other parts together. The ceramic rings and high-voltage connections would be protected from seawater by enclosing those parts of the transducer in an oil-filled volume. This oil-filled portion of the transducer is defined by elastomer boots; one inside the cavity and one over the outside diameter of the transducer. To minimize the in-air weight of the device, the oil-filled volume is minimized and all metal parts are anodized aluminum.

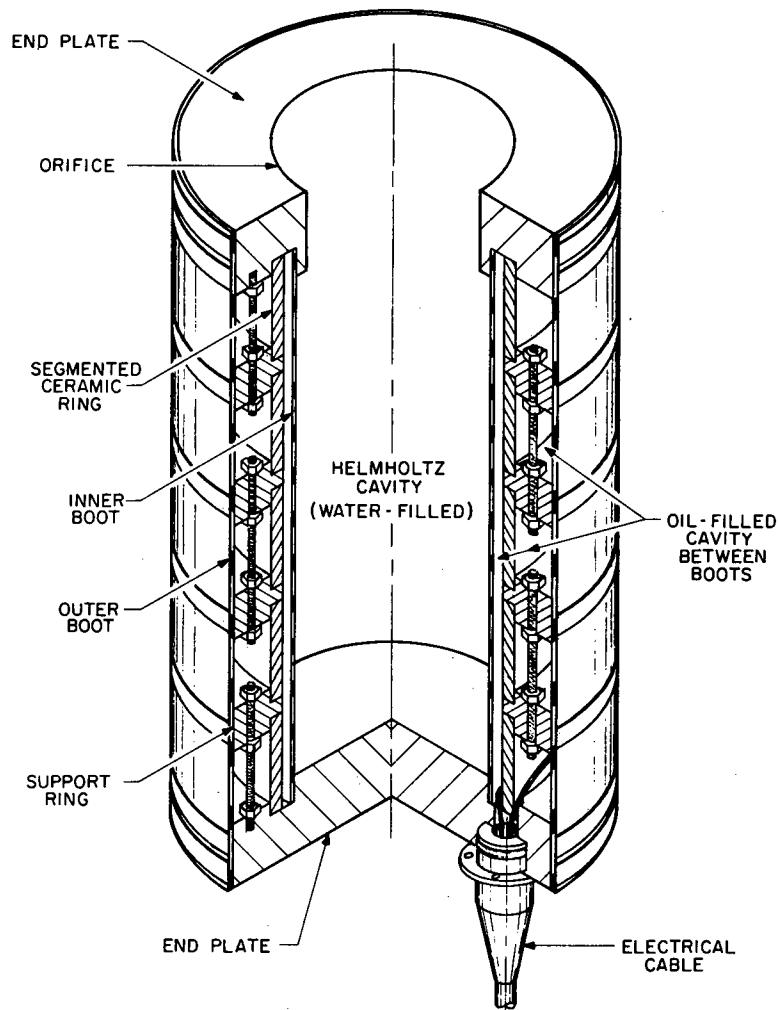


Fig. 3 — Conceptual design for a low-frequency, high-power, deep-towed transducer.

ANALYSIS OF THE SUBJECT TRANSDUCER

The electro-mechano-acoustical circuit shown in Fig. 4 describes the conceptual design for a Helmholtz resonator to meet the requirements of the deep-towed application and was developed from the various masses, compliances, resistances, and radiation impedances associated with the transducer. The electromechanical *turns ratio*, N , transforms an applied voltage into a corresponding force and is

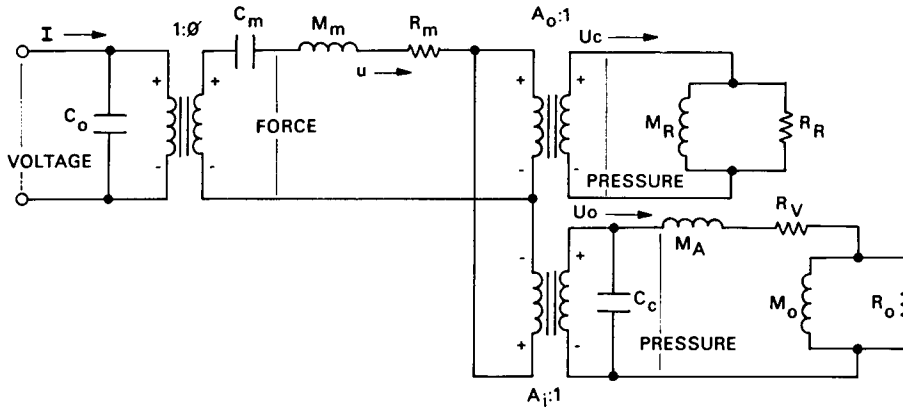


Fig. 4 — Electro-mechano-acoustical circuit for a Helmholtz resonator

dependent upon the geometry of the ceramic driver and the material from which it is made. There are, of course, two radiators associated with this type of transducer; the surface of the ceramic rings exposed directly to the medium and the fluid *piston* moving in the orifice. The radiation impedances acting on these two *surfaces* are coupled to the mechanical portion of the circuit by the area transformations, A_o and A_i ; where A_o represents the outside surface area of the ceramic driver and A_i is the inside surface area of the driver. The individual elements in the equivalent circuit are: C_o is the blocked capacitance of the ceramic driver; C_m , M_m , and R_m are the mechanical compliance, mass, and resistance of the ceramic driver, respectively; M_r and R_r represent the radiation impedance acting on the outer surface of the driver; C_c is the acoustic compliance of the cavity; M_A is the acoustic inertance of the orifice; R_v is the viscous loss associated with the motion of fluid in the cavity; and M_o and R_o represent the radiation impedance acting on a piston at the end of a long tube with an inside radius equal to that of the orifice. The currents U_c and U_o represent the volume velocities associated with the radiation from the outer surface of the ceramic and orifice respectively; u is the linear velocity; and I , of course, is the electrical current.

If the transducer is assumed to be small when compared to the acoustic wavelength in water, removing the electromechanical and mechano-acoustical transformers results in the simplified equivalent circuit shown in Fig. 5. M_I is an *inertial* term representing the fact that the volume flow emanating from the orifice has two effects: the desired radiation of acoustic energy from the orifice and the undesired acceleration of the transducer structure. This term, therefore, appears in the circuit as a shunt impedance around the radiation resistance.

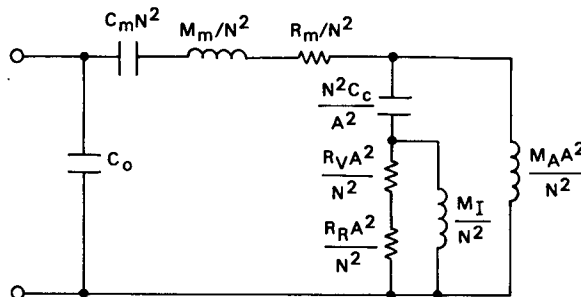


Fig. 5 — Simplified equivalent circuit for the Helmholtz transducer

The values of the elements in the equivalent circuit are, of course, dependent upon the dimensions of the transducer and the materials used in its construction. In previous discussions, it was decided to maximize the diameter of the transducer with the geometry constraints of the application and then vary the length to achieve the desired resonance frequency. As previously stated then, the radius of the orifice, a_o , is equal to the inside radius of ceramic rings, a_i ; however, the cavity length required for the desired resonance frequency still must be determined.

Equation (1) can be more correctly stated as

$$f_r = \frac{1}{2\pi} \sqrt{\frac{1}{C_T M_A}}, \quad (3)$$

where the total compliance, C_T , is the sum of the cavity compliance, C_c , and the compliance of the shell formed by the piezoelectric rings, C_m . For a tube rigidly closed on one end, the acoustic impedance acting on the open end is given by [6]

$$Z_a = -j \frac{\rho_o c}{\pi a_i^2} \cot(kl), \quad (4)$$

where ρ_o is the density and c is the sound speed of the medium respectively; a_i is the inside radius of the tube; $k = \frac{\omega}{c}$, ω is the frequency in radians; and l is the length of the tube. If the cotangent term in Eq. (4) is replaced by its series representation and the results rearranged, then

$$Z_a = j \left\{ \frac{\omega l \rho_o}{3\pi a_i^2} \left[1 + \left(\frac{\omega l}{c} \right)^2 \frac{1}{15} + \left(\frac{\omega l}{c} \right)^4 \frac{2}{315} + \dots \right] - \frac{1}{\omega} \left(\frac{\rho_o c^2}{l\pi a_i^2} \right) \right\}, \quad (5)$$

which is of the form $Z_a = j(\omega M_a - 1/n\omega C_a)$, where M_a is the acoustic mass or inertance and C_a is the acoustic compliance. From Eq. (5) the acoustic compliance of the cavity is $l\pi a_i^2/\rho_o c^2$ and the inertance, for the first four terms of the cotangent expansion, is given by

$$M_a = \frac{l' \rho_o}{3\pi a_i^2} \left\{ 1 + \left(\frac{\omega l'}{c} \right)^2 \frac{1}{15} + \left(\frac{\omega l'}{c} \right)^4 \frac{2}{315} \right\}, \quad (6)$$

where l' now represents the actual length of the tube plus some end correction and a_i is the orifice radius.

The mechanical compliance of the cylindrical shell formed by the ceramic rings can be found from

$$C_m = \frac{S_{33}^E a_m}{2\pi l_c t_c}, \quad (7)$$

where S_{33}^E is the reciprocal elastic modulus of the ceramic material (i.e., the reciprocal of Young's modulus), a_m is the mean radius of the ceramic rings, l_c is the total length of the ceramic shell, and t_c is the wall thickness of the ceramic rings. To arrive at an equation for the required cavity length, the expressions for the cavity compliance, the compliance of the shell (in acoustical units), and the inertance (Eq. (6)) can be substituted into Eq. (3) and rearranged in terms of l . The result is a fourth order polynomial in l where the coefficients are dependent upon the ceramic material, the transducer dimensions, and the desired resonance frequency. Once the cavity length is determined, the value of the individual circuit elements may be calculated and the techniques of electrical circuit analysis applied.

The primary parameter of interest in this case is the transmitting voltage response (TVR) of the transducer (i.e., the radiated sound pressure level per volt applied to the transducer as a function of frequency). The acoustic pressure generated by the transducer at a distance r can be obtained from

$$p = (1/r) (P_A \rho_o c R_\theta / 4\pi)^{1/2}, \quad (8)$$

where P_A is the radiated acoustic power and R_θ is the directivity factor. By definition, TVR is referenced to a measurement distance of one meter and for most of the frequency range under consideration the directivity factor may be assumed to equal unity. In terms of the simplified equivalent circuit the radiated acoustic power is analogous to the power dissipated in the radiation resistance. After substitution of nominal value for ρ_o and C , the conversion to the proper standard units (micropascals), Eq. (8) may be rewritten as

$$p = (345.494 \times 10^6) (P_R)^{1/2}, \quad (9)$$

where P_R is the power dissipated in the radiation resistance, R_R . The TVR then, can be obtained from Eq. (9), the current in the radiation resistance branch of the circuit, and the value of the radiation resistance.

Although all of the analysis to this point has been for the case where the orifice diameter is equal to the inside diameter of the cavity, that condition cannot actually be realized in any practical design. The requirement for an inner boot naturally implies some means of mechanically fastening that boot to each end of the transducer cavity with the end result being an unavoidable reduction in the diameter of the open end of the tube. The primary effect of such a reduction will be a shift in the Helmholtz resonance frequency. Looking at the parameters which directly affect the resonance frequency (Eq. (3)), only the inertance M_A is directly dependent upon the orifice size. The frequency shift is downward since the inertance is inversely proportional to the square of the orifice radius; that is, the shift in the resonance frequency is directly proportional to the ratio of the actual orifice to the inside radius of the cavity. As long as the length of the actual orifice remains small, any increase in viscous loss can be neglected. In the case of this design, the metal ring needed to attach the inner boot at the orifice end of the cavity is a reasonable approximation of a thin plate and its effective length may be assumed to be zero.

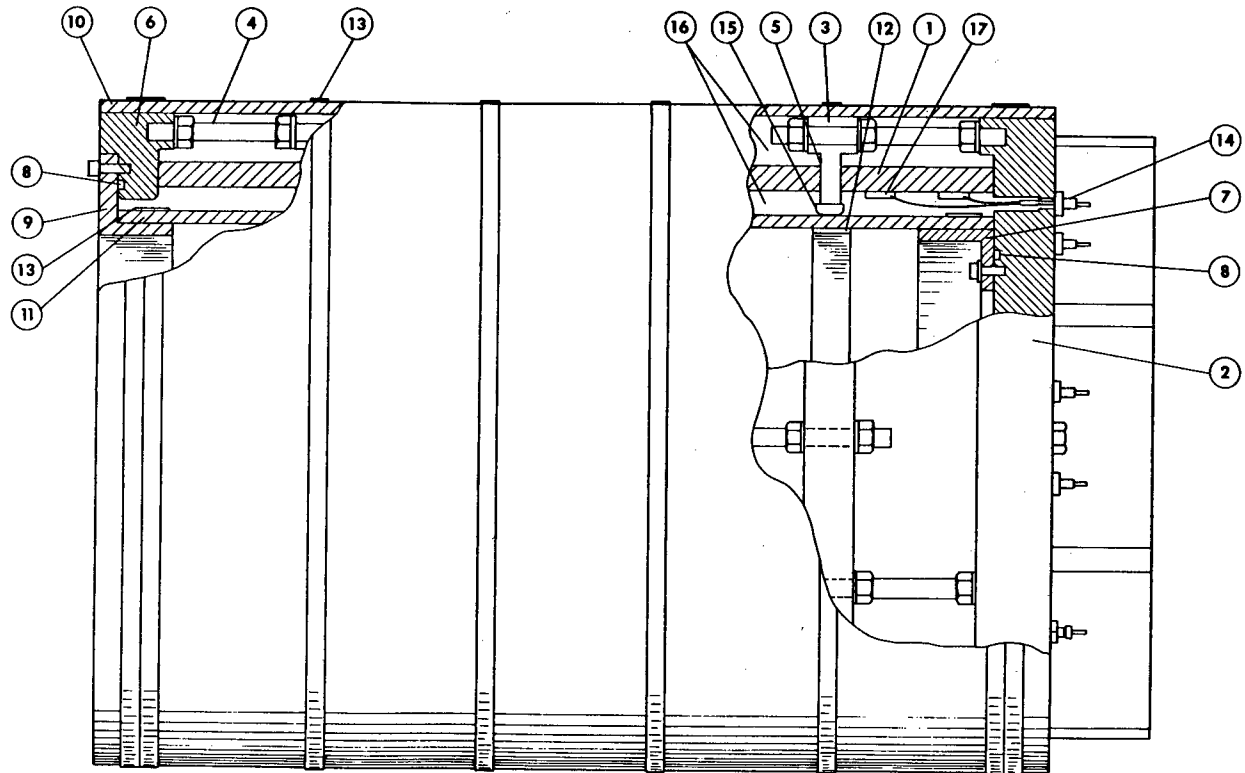
To the best of our knowledge, this effort represents the first time that a Helmholtz resonator has been used to meet the combined requirements of broad operational bandwidth at low frequencies, unlimited depth capability, and high output power. Due to the tight delivery schedule required, the costs involved and the element of risk that accompanies any initial development, a scale model of the transducer was built and evaluated in an attempt to verify the analysis and the fabrication techniques suggested in the conceptual design. The scale factor (4.38:1) was determined by the diameter of available piezoelectric ceramic rings, and to the extent possible, the model was a scaled replica of the transducer shown in the conceptual design of Fig. 3. Since the cavity diameter was fixed by the ceramic rings, the cavity length required for the scaled Helmholtz resonance frequency (~ 1300 Hz) was determined by the procedure previously outlined, assuming the end correction is that of an unflanged tube [6, p. 133]. The simplified equivalent circuit shown in Fig. 5 was used to compute the TVR and equivalent series impedance of the scale model and the results were compared with measured values. The scale model proved to be an extremely useful design tool and led to several significant conclusions: the method of calculating the cavity length and the simplified equivalent circuit were proven to be correct; subtle assembly techniques were developed and verified; the significance of the transducer mass was demonstrated; unexpectedly, the estimation of the viscous loss was shown to be inadequate; and it was discovered that aluminum was an unsuitable material for the spacer rings in the support framework. The model used for the viscous loss simply considered oscillating flow over a large surface and did not take into account the shape of the cavity or any effects of the inner boot on cavity loss. No analytical method for calculating the total cavity loss has been found and other investigators have encountered the same difficulty [4, p. 8]. Since the Q of the cavity (or the cavity loss) predominantly affects the Q of the transducer at resonance, it is relatively unimportant in this broadband application. In the scale model transducer the aluminum spacer rings were found to be vibrating out of phase with the ceramic rings; in other words, they were too compliant. The net effect was a resonance frequency slightly lower than expected and a reduction in the output sound pressure level. The only practical way to increase the stiffness of the rings and still keep the outside diameter of the transducer at a minimum, was to change to a stiffer material. New spacer rings of the same dimensions were fabricated from mild steel

(a three-fold increase in stiffness) and the problem was solved. The penalty to be paid was the corresponding increase in transducer weight.

ELECTROMECHANICAL DESIGN

Guidelines for the design of the subject transducer can be developed by considering the conclusions of the previous two sections. The desire for a large cavity volume leads to the conclusion that the diameter of the ceramic rings should be maximized within the constraints of the specifications. In order to minimize the viscous loss in the orifice, the orifice diameter should be as close to the inside diameter of the cavity as possible (i.e., the diameter of the inner boot should be as large as possible). The cavity length required for the desired resonance frequency may be determined from the previous analysis, but to obtain the highest possible TVR, the volume of piezoelectric ceramic in the transducer should be maximized; in other words, as much of the cavity length as possible should be formed by the ceramic rings.

Application of these guidelines leads to the detailed design shown in the sectioned drawing of Fig. 6. As shown, the USRD type G62 transducer measures approximately 0.7 m o.d., 1.1 m long, and weighs approximately 800 kg in air. The Helmholtz cavity is 0.92 m long with an orifice diameter of



- | | |
|---|--|
| 1 Prestressed parallel mode Type I ceramic ring | 9 Orifice inner boot ring |
| 2 Aluminum back plate with reinforcement ribs | 10 Outer boot |
| 3 Steel spacer ring | 11 Inner boot |
| 4 1.91-cm-dia steel rods with lock washers and locking nuts | 12 Inner boot stabilizing ring |
| 5 Polyethylene-terephthalate (Mylar) insulator with industrial adhesive | 13 Stainless steel banding |
| 6 Aluminum orifice end ring | 14 Independent bulkhead connectros (Mecca) for each ring |
| 7 Back plate inner boot ring | 15 Rubber bumpers |
| 8 O-ring seals | 16 Castor oil fill-fluid |
| | 17 Nickel electrode tabs with hook-up wire |

Fig. 6 — Sectional view of USRD type G62 transducer

0.42 m. Approximately 85% of the cavity length is formed by 275 kg of NAVY Type I [7] lead-zirconate-titanate piezoelectric ceramic divided into five segmented rings. Each ring has an o.d. of 56 cm, a wall thickness of 2.5 cm, and a length of 15.5 cm. Based upon these dimensions and the properties of the materials used, values for the elements in the simplified equivalent circuit of Fig. 5, were computed (the values used and their derivations are shown in Appendix A). The equivalent circuit was then used to calculate the theoretical TVR of the transducer for two different orifice radii. The expected TVR with the orifice radius, a_o , equal to the inside radius of the cavity, a_i , and with the orifice radius equal to $(0.825) a_i$, the actual dimension, are both shown in Fig. 7.

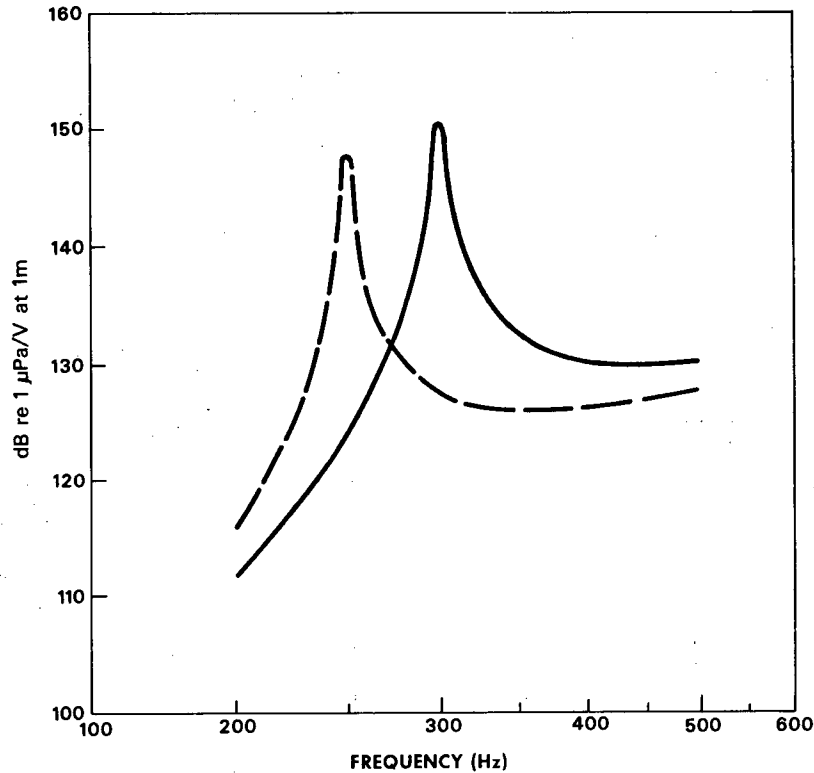


Fig. 7 — Predicted transmitting voltage response for an orifice radius equal to the inside radius of the cavity (solid line); for an orifice radius equal to $0.825 \times$ inside radius (dashed line).

Each of the ceramic rings is formed by the consolidation of 96 stave sections or bars with 50% voided nickel foil electrodes interposed between the staves. This consolidation is accomplished using industrial adhesive and each finished ring is mechanically prestressed by a circumferential wrap of glass-fiber/epoxy composite. A finished ceramic ring is shown resting on the transducer back plate in Fig. 8.

The electrical parameters of six segmented ceramic rings, five of which were used in the construction of the G62, are shown for the conditions of before and after mechanical prestressing in Table 2. The before and after data were measured by the ceramics manufacturer and the after data was confirmed by measurements at USRD. The theoretical capacitance of a parallel mode segmented ring is given by

$$C = \frac{\epsilon_o K_{33}^T n^2 l}{2\pi} \log_e(b/a), \quad (10)$$

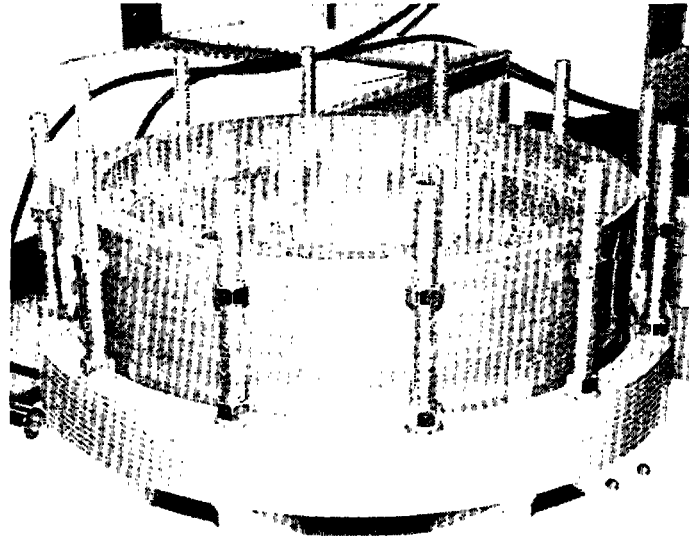


Fig. 8 — Finished piezoelectric ceramic ring resting on the transducer back plate.

Table 2 — Electromechanical Properties of G62 Ceramic Rings

	Ring Number	Capacitance @100 Hz ($\times 10^{-7} F$)	Dissipation (%)	Resistance (10^9 ohms)	f_r (Hz)	R_r (Ω)	f_a (Hz)	R_a ($k \Omega$)	k_{33}^2 *	Q_m **
Before Prestress	1	2.70	0.5	2.0	1680	—	2150	—	0.389	—
	2	2.54	0.5	1.0	1647	—	2151	—	0.414	—
	3	2.48	0.4	1.0	1684	—	2150	—	0.387	—
	4	2.46	0.6	1.0	1694	—	2189	—	0.401	—
	5	2.61	0.5	1.0	1685	—	2169	—	0.396	—
	6	2.53	0.5	1.1	1686	—	2151	—	0.386	—
	mean	2.55	0.5	1.2	1679	—	2160	—	0.396	—
	STD \pm	0.09	0.06	0.4	16.5	—	16	—	0.011	—
After Prestress	1	2.768	0.33	1.6	1777	5.9	2164	37	0.326	168
	2	2.684	0.25	2.0	1788	5.0	2190	33	0.333	199
	3	2.759	0.21	1.5	1766	4.2	2185	35	0.347	224
	4	2.719	0.31	1.1	1773	3.6	2222	35	0.363	250
	5	2.677	0.36	2.0	1757	3.8	2196	36	0.360	257
	6	2.588	0.26	1.5	1771	4.7	2183	41	0.342	216
	mean	2.699	0.29	1.6	1772	4.53	2190	36.2	0.345	217
	STD \pm	0.066	0.06	0.3	10	0.85	19	2.7	0.015	33

$$* k_{33}^2 = \frac{f_a^2 - f_r^2}{f_a^2}$$

$$** Q_m = \frac{f_a^2}{W_o C_r R_r (f_a^2 - f_r^2)}$$

where ϵ_o is the permittivity of free space; K_{33}^T is the free relative dielectric constant of the ceramic; n is the number of staves in the ring; l is the length of the ring; and b is the outside radius of the ring while a is the inside radius. The computed capacitance of a single ring, 2.49×10^{-7} Farads compares favorably with the mean capacitance of the six rings shown in Table 2 (before prestress).

Under conditions of high electrical drive, the magnitude of the ceramic motion can be large enough to exceed the tensile strength of the material. To prevent the possibility of a tensional fracture of the ceramic, the rings must be mechanically prestressed to ensure that they remain in compression. This can be accomplished by circumferentially winding glass filament under tension onto the ceramic ring to produce a constant compressional stress in the material. The magnitude of this bias prestress should be at least equivalent to the stress produced in the material by the maximum expected driving voltage. Care should be taken, however, not to prestress the ceramic more than necessary because over stressing can significantly alter the piezoelectric and mechanical properties of the rings.

One approach which may be used to determine the prestress magnitude is to consider the ring as an acoustic receiver and then find the sound pressure level required to produce an output voltage equal to the maximum driving voltage. The theoretical free-field voltage sensitivity (FFVS) of a circumferentially poled ring of n segments is given by

$$\frac{V}{P_o} = \frac{2\pi b}{n \log_e(\rho_0)} \left\{ g_{31} \left[\gamma(1 - \rho) + \frac{1 - \rho}{1 + \rho} (\beta + \rho\alpha) \right] + g_{33}(\beta - \rho\alpha) \right\}, \quad (11)$$

where ρ is the ratio of the inside to outside radii, a/b ; g_{31} and g_{33} are piezoelectric constants of the ceramic; and α , β and γ represent the boundary conditions of the inside, outside, and end surfaces of the rings respectively (that is, $\alpha = \beta = \gamma = 1$ for the exposed surfaces and $\alpha = \beta = \gamma = 0$ for shielded surfaces) [8]. For the dimensions and configuration ($\alpha = \beta = 1$ and $\gamma = 0$) of the rings in the G62, the theoretical FFVS, is approximately -192 dB referenced to 1 V per μPa ; in other words, a sound pressure level of 192 dB referenced to 1 μPa impinging on the ring would produce an output voltage of 1 V. The minimum and maximum prestress desired are determined from the maximum expected driving voltage and an acceptable margin of safety, respectively. The maximum expected driving voltage for the G62 is 5000 V and a reasonable safety margin is 1000 V (6000 V total) which translate into prestress limits of 20 to 24 MPa.

As seen in Fig. 6, the support framework for the G62 consists of the back plate, four spacer rings, the orifice end ring, and the threaded rod, nuts, and washers required to fasten the other parts together. The back plate, orifice end ring, the back plate inner boot ring, and the orifice inner boot ring (all the parts exposed to salt water) are fabricated from aluminum and hard coat anodized. Because of the required mechanical stiffness, the spacer rings and fasteners are steel and are enclosed in the oil-filled volume between the elastomer boots. The back plate is stiffened by the addition of welded aluminum ribs.

In the transducer assembly, the ceramic rings must be supported, but not mechanically clamped, by the framework. In addition, a somewhat contradictory requirement is that to maintain the required cavity compliance and resonance frequency, there can be no acoustic path between the fluid-filled cavity and the surrounding medium, except through the orifice. In other words, there can be no clearance between the ends of the ceramic rings and the mating surfaces of the support framework. Both of these objectives were accomplished during construction by using a two-step procedure. The ends of each ceramic ring were coated with industrial adhesive used in this case as a grout or filler rather than a bonding agent (i.e., adhesive is used to fill any gaps or unevenness between the staves at the ends of the ceramic rings). An 0.8-mm-thick ring of polyethylene-terephthalate is placed between the coated ends of the ceramic and the mating metal parts as an electrical insulator and the subassembly is longitudinally *compressed* while the adhesive cures. This compression is achieved by placing a mass of approximately 100 kg on the spacer-ceramic ring subassembly causing the adhesive to flow into any existing gaps at the ends of the ring. The adhesive is prevented from bonding to the metal parts by the

polyethylene insulator. After the adhesive has cured, the metal parts of the framework on either side of the ceramic are fastened together by the support rods *without* adding any additional compressive stress beyond that of the 100 kg *dead weight*. The point is, while the 100 kg is sufficient to ensure intimate contact between the ceramic and the mating parts, it is not large enough to mechanically clamp the ceramic ring. Starting with the first ring on the transducer back plate, this *grouting* and *weighting* procedure is continued for each ceramic ring until all five are in place. The outside diameter of the ceramic ring is prevented from moving into contact with the inside diameter of the steel spacer ring by elastomer spacers on the circumference of the ceramic. There is more than enough clearance for the ceramic to vibrate freely, the intent of the spacers is to keep the ceramic centered in the event of mechanical shock perpendicular to the longitudinal axis of the transducer. The ceramic stack is shown in various stages of assembly in the photographs of Fig. 9.

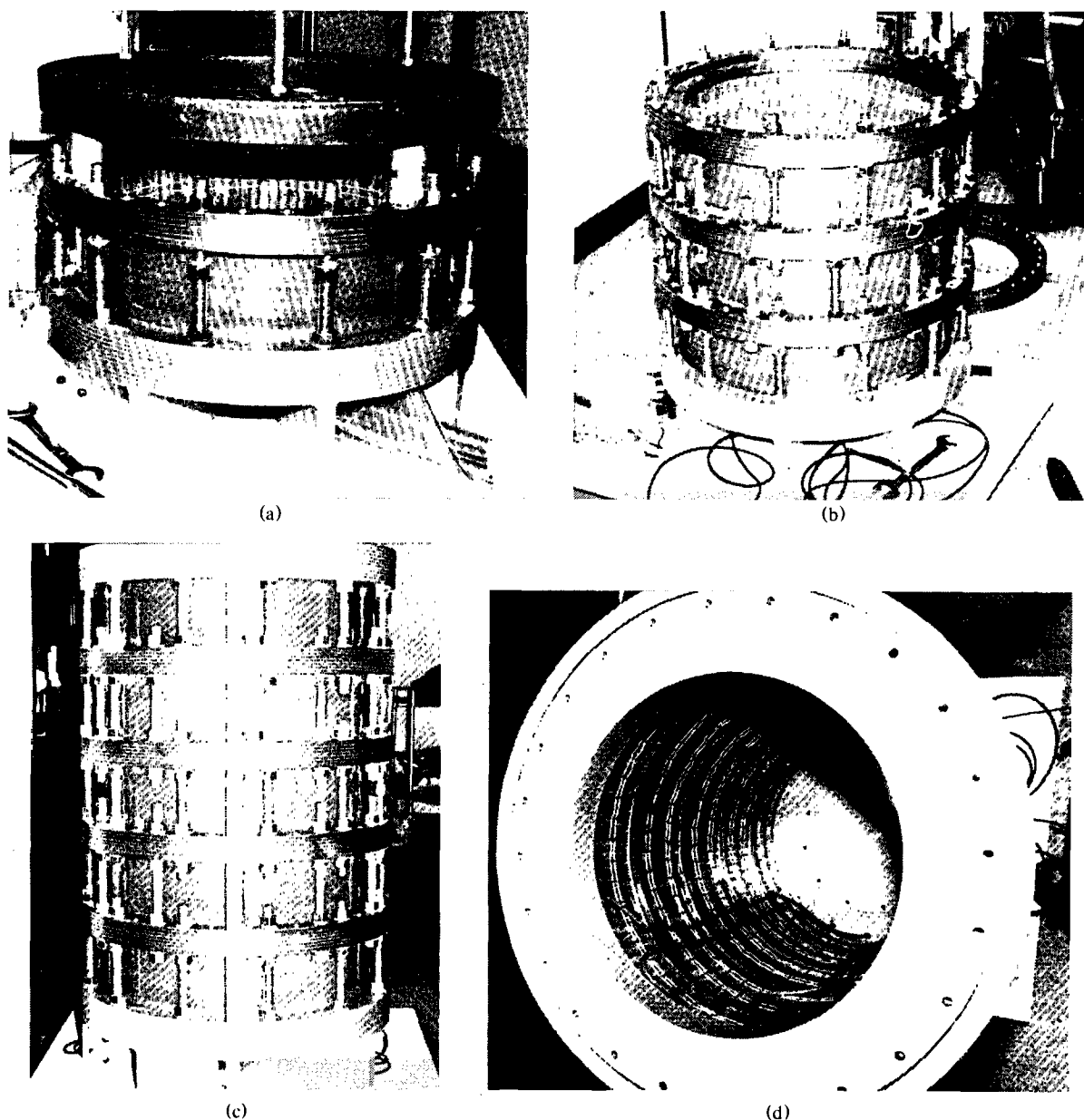


Fig. 9 — Construction of the USRD type G62 transducer: (a) Installation of the first spacer ring with "dead weight," (b) Installation of the first three ceramic rings, (c) Side view of the completed transducer without boots, and (d) View of the orifice end of the transducer before boot installation.

The two electrical leads for each ring are routed to individual bulkhead connectors on the transducer back plate with high-voltage silicone-jacketed hookup wire. To prevent failure due to metal fatigue, the points of connection to the nickel foil electrodes are potted in place with industrial adhesive and the connections between individual staves in each ring are accomplished with a beryllium copper alloy wire. The high voltage sections of the transducer are enclosed within the oil-filled volume between the boots.

The outer boot is 1.6 cm thick while the inner boot is 1.3 cm thick; both are molded from a neoprene elastomer. The outer boot is held in place by stainless steel bands at the back plate, the orifice end ring, and at each of the spacer rings. The inner boot is banded to a boot mounting ring at each end, which in turn are fastened to the transducer back plate and orifice end ring. The shape of the inner boot is maintained by placing four stainless steel stabilizing rings inside of the boot and banding them in place at locations along the length corresponding to the spacer rings in the support framework. Molded rubber *bumpers* are attached to the i.d. of the spacer rings and are used to *capture* the inner boot against the stabilizing rings. The transducer was placed in a vacuum chamber and the volume between the boots was filled with castor oil. The completed transducer is shown mounted in its handling fixture in Fig. 10.

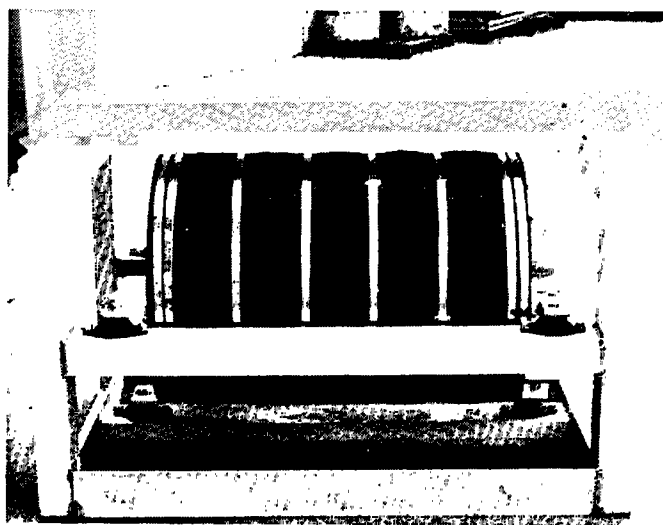


Fig. 10 — The completed transducer mounted in its handling fixture

ACOUSTIC EVALUATION OF THE G62 TRANSDUCER

The completed transducer was evaluated at the USRD Leesburg Facility at water depths to 31 m. Characteristics measured included TVR, equivalent series impedance, and linearity as a function of driving voltage. Directivity was measured in the horizontal XY plane with the transducer mounted in the handling fixture; directivity patterns were measured in both the horizontal XY and vertical XZ planes with the transducer mounted in the NORDA tow body.

The measured TVR is compared with that predicted by the equivalent circuit model in the curves of Fig. 11. As seen in this figure, the agreement between the measured and theoretical responses is quite good at all frequencies except those in the immediate vicinity of the Helmholtz resonance. Obviously, the damping or loss in the system is considerably greater than that predicted by the equivalent circuit model. The only damping term in the equivalent circuit is the viscous loss in the cavity and it does not appear reasonable that it alone is responsible for the relatively large discrepancy. A far more

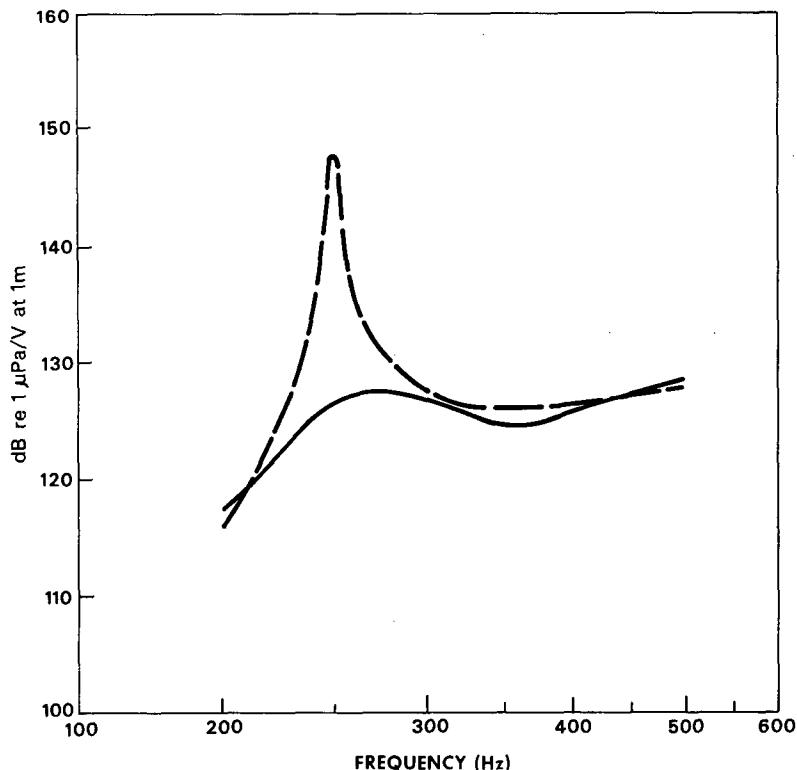


Fig. 11 — Comparison of the measured TVR of the G62 transducer (solid line) with that predicted by the equivalent circuit model (dashed line).

reasonable explanation centers around a portion of the transducer not included in the equivalent circuit model, the elastomer inner boot. While it was recognized that the inner boot represented a possible loss mechanism, no attempt was made to model it because of the great difficulty involved in attempting to arrive at an accurate representation. At any rate, the highly damped resonance may be shown to be not only relatively unimportant, but actually an advantage for this application. Since the intended application is for a broad bandwidth device, obtaining a high efficiency, or a high Q , at resonance is of little importance. The highly damped resonance may be considered an advantage in that it provides a margin of safety; that is, even at the maximum applied voltage (5000 V) the sound pressure level limit set by the fracture stress of the ceramic cannot be reached. The over-damped resonance actually produces a response which is flat (± 2 dB) over the entire operating frequency range while still providing a *boost* of approximately 12 dB over the ceramic alone at the low frequencies.

The measured and predicted equivalent series impedance are compared in Fig. 12 and, not surprisingly, shows the same large difference in damping or loss. The reactive portion of the impedance, however, is reasonably well predicted. The large reactive component of the impedance is a primary disadvantage of this type of transducer.

For this specific application, a special power amplifier and matching network were designed by NORDA, but were not interfaced with the transducer for these measurements. Although the transducer can safely withstand 5000 V, the maximum voltage applied was limited to approximately 1000 V by the available power amplifier. Measurements to this point indicate that the sound pressure level is linear to within 1 dB for drive voltages up to this level.

With the transducer mounted in the handling fixture, the directivity patterns in the horizontal XY plane are all omnidirectional (± 1.5 dB) except at the higher frequencies; the directivity pattern at 500 Hz is shown in Fig. 13. The directivity patterns at some frequencies were distorted somewhat when the

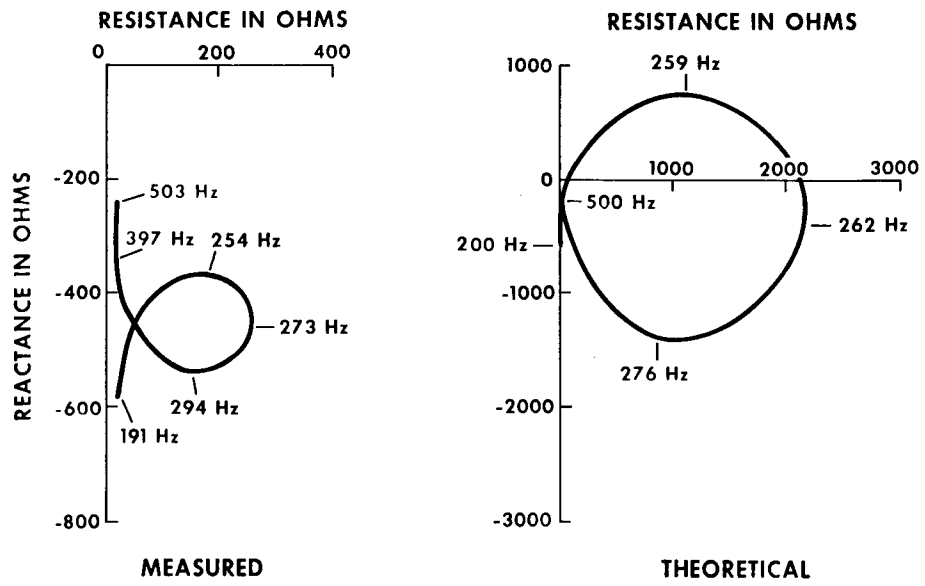


Fig. 12 — Comparison of the measured and theoretical equivalent series impedance of the G62 transducer

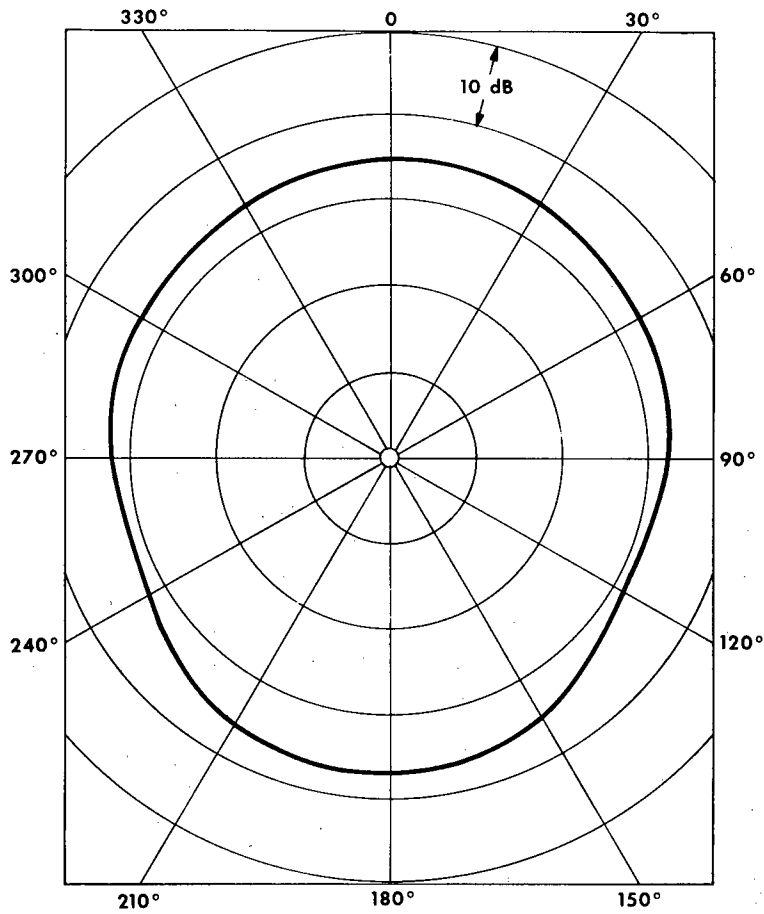


Fig. 13 — Horizontal (XY) directivity pattern of the G62 transducer mounted in the handling fixture at 500 Hz

transducer was mounted in the tow body, but the decisions of acceptable directivity and possible modifications to the tow body were left to the user, NORDA.

In December 1981, the transducer was installed in an experimental DTAGS system and loaded aboard the USNS *Lynch* for at-sea evaluation in the Gulf of Mexico. No changes were detected in the transducer's characteristics when it was exposed to drive voltages of nearly 2000 V and depths of over 2000 m. The transducer is presently awaiting installation in a revised experimental DTAGS system to be evaluated during 1982.

CONCLUSIONS

The piezoelectrically driven Helmholtz resonator can be configured to a low-frequency, high-power acoustic source which is insensitive to hydrostatic pressure, although trade-offs must be made between bandwidth and physical size for any given application. The requirement for supplying a large amount of reactive power may be reduced by electrical tuning at the expense of bandwidth. Further work is required in the modeling of such devices particularly in the area of obtaining accurate estimates of the Q of the Helmholtz cavity in various configurations.

In general, all low-frequency, high-power sources are large, heavy, and necessarily inefficient; and bandwidth and efficiency decrease as a function of increasing depth requirements. At any rate, no one transducer exists which is suitable for all low-frequency needs, and there are applications to which the piezoelectric Helmholtz resonator is well suited.

ACKNOWLEDGMENTS

The authors are indebted to several USRD staff members for their assistance in the successful development of this transducer: G.D. Hugus assisted in the mechanical design; the many assemblies and disassemblies of the scale model were accomplished by J.G. Williams; and valuable assistance was provided during the assembly and evaluation phases of the work by M.D. Jevnager.

REFERENCES

1. G. Fagot and B.G. Eckstein, "Deep-Towed Geophysical Array Development Program Progress Report (FY1978)," NORDA Technical Note 41, February 1979.
2. I.D. Groves and T.A. Henriquez, "Electroacoustic Transducers for a 10,000-psig Underwater Sound Transducer Calibration Facility for the Frequency Range 10 to 4000 Hz," NRL Report 6967, 15 Aug 1969 [AD-693051].
3. T.A. Henriquez, "The USRD Type F39A 1-kHz Underwater Helmholtz Resonator," NRL Report 7740, 10 Apr 1974.
4. R.S. Woollett, "Underwater Helmholtz Resonator Transducers: General Design Principles," NUSC Technical Report 5633, 5 Jul 1977.
5. T.A. Henriquez and A.M. Young, "The Helmholtz Resonator as a High-Power Deep-Submergence Source for Frequencies below 500 Hz," *JASA* **67**, p. 1555 (1980).
6. L.L. Beranek, *Acoustics*, (McGraw-Hill, New York, 1954) pp. 128-129.
7. "Piezoelectric Ceramic for Sonar Transducers," MIL-STD-1376 (SHIPS) (U.S. Government Printing Office, Washington, DC, 1970).
8. D.W. Wilder, "Electroacoustic Sensitivity of Ceramic Cylinders," *JASA* **62**, p. 769 (1977).

Appendix A
DETERMINATION OF VALUES FOR THE ELEMENTS
OF THE G62 EQUIVALENT CIRCUIT

Figure 5 of this report shows the simplified equivalent circuit for the G62 transducer. The values for the elements of that equivalent circuit are dependent upon the geometry of the transducer, the materials used in its construction, and, in some cases, the frequency. The dimensions and material properties of interest for the G62 are listed in Table A1.

The symbols " N " and " A " in the equivalent circuit represent the *turns ratios* of electromechanical and mechanoacoustical transformers; that is, N^2 transforms mechanical to electrical impedances while A^2 transforms acoustical to mechanical impedances. Therefore, N can be written in terms of the geometry of the ceramic driver and its piezoelectric properties as

$$N = \frac{2\pi n t_c l_c d_{33}}{\pi D_{\text{mean}} S_{33}^E}, \quad (\text{A1})$$

substituting from Table A1, yields,

$$N = 132.9 N/V.$$

For this simplified circuit, the area transformation is taken to be the mean area of the cylindrical ceramic driver, or

$$A = 2\pi a_m l_c = 1.54 \text{ m}^2. \quad (\text{A2})$$

The first element in the circuit is the "blocked" capacitance of the ceramic driver, C_o .

The capacitance of a single ceramic ring is given in the test by Eq. (9) as

$$C = \frac{\epsilon_o K_{33}^T \ln^2}{2\pi} \log_e \left(\frac{a_o}{a_i} \right), \quad (\text{A3})$$

where l is the length of one ring. If l is replaced by the length of the ceramic driver, l_c , the same equation yields the capacitance for all five rings in parallel. Again substituting values from Table A1,

$$C_o = 1.24 \times 10^{-6} \text{ F}. \quad (\text{A4})$$

The mechanical compliance is written in terms of the geometry and elastic properties of the material in the shell forming the ceramic,

$$C_m = \frac{a_m S_{33}^E}{2\pi t_c l_c} = 2.716 \times 10^{-11} \text{ M/N}; \quad (\text{A5})$$

therefore,

$$C_m N^2 = 4.797 \times 10^{-7} \text{ F}.$$

The mechanical mass is simply the mass of the ceramic driver, or

$$M_m = \rho_m [\pi l_c (a_o^2 - a_i^2)] = 249.0 \text{ kg} \quad (\text{A6})$$

Table A1 — Constants for the Calculation of Equivalent Circuit Elements for the G62 Transducer.

<u>CHARACTERISTICS OF THE CERAMIC DRIVER</u>	
Outside Radius, a_o	0.279 m
Inside Radius, a_i	0.254 m
Mean Radius, a_m	0.267 m
Wall Thickness, t_c	0.025 m
Length of Ceramic (5 Rings), l_c	0.775 m
Density of Ceramic, ρ_m	7550 kg/m ³
Mechanical Q , Q_m	
Piezoelectric Constant, d_{33}	280×10^{-12} m/V
Reciprocal Modulus, S_{33}^E	1.493×10^{-11} m ² /V
Number of Segments Per Ring, n	96
<u>DIMENSIONS OF THE CAVITY</u>	
Cavity Length, l_{cav}	0.919 m
Orifice Radius, a_{or}	0.210 m
<u>FLUID PROPERTIES</u>	
Density of Water, ρ_o	1000 kg/m ³
Sound Speed in Water, C_o	1500 m/s
Density of Castor Oil, ρ	950 kg/m ³
Sound Speed in Castor Oil, C	1540 m/s
Coefficient of Viscosity, Castor Oil, η	0.986 kg/m · s

and

$$\frac{M_m}{N^2} = 1.41 \times 10^{-2} H.$$

The mechanical resistance is expressed in terms of the dimensions and mechanical properties of the ceramic driver

$$R_m = \frac{a_m (\rho_m S_{33}^E)^{1/2}}{Q_m C_m} = 6.588 \times 10^3 \frac{N \cdot s}{m} \quad (A7)$$

$$\frac{R_m}{N^2} = 0.373 \text{ ohm.}$$

The acoustical compliance of the cavity is

$$C_c = \frac{\pi a_i^2 l_{cav}}{\rho_o C_o^2} = 8.276 \times 10^{-11} \frac{M^5}{N}$$

and

$$\frac{C_c N^2}{A^2} = 6.167 \times 10^{-7} F. \quad (A8)$$

The *inertial mass* of the transducer is simply the estimated weight of the transducer in water

$$M_I = 600 \text{ kg}, \quad \frac{M_I}{N^2} = 3.397 \times 10^{-2} H. \quad (A9)$$

The remaining three elements in the circuit, the viscous loss, the radiation resistance and the inertance of the orifice, are all frequency dependent. The viscous loss is taken to be simply the loss due to viscous flow over a large surface

$$R_v = (\pi \eta \rho f)^{1/2}. \quad (A10)$$

From the values listed in the table,

$$R_v = 54.247 f^{1/2} N \cdot s / m^5$$

and

$$\frac{R_v A^2}{N^2} = (7.284 \times 10^{-3}) f^{1/2} \text{ ohms.} \quad (A11)$$

The radiation resistance used in this case is that for a radially vibrating cylinder

$$R_R = \frac{\rho_o C_o}{2\pi a_o l_c} \frac{(2ka_o)^2}{1 + (2ka_o)^2} = \frac{6.043 f^2}{1 + (5.479 \times 10^{-6}) f^2} \frac{N \cdot s}{m^5} \quad (A12)$$

$$\frac{R_R A^2}{N^2} = \frac{(8.114 \times 10^{-4}) f^2}{1 + (5.479 \times 10^{-6}) f^2} \text{ ohms.}$$

The inertance or acoustical mass of the orifice is given by Eq. (6) in the text. Substituting values from the table yields,

$$M_A = 2.117 \times 10^3 \{1 + (1.390 \times 10^{-6}) f^2 + (2.760 \times 10^{-12}) f^4\} \frac{\text{kg}}{M^4}$$

and

$$\frac{M_A A^2}{N^2} = \{0.292 + (4.063 \times 10^{-7}) f^2 + (8.068 \times 10^{-13}) f^4\} H. \quad (A13)$$